

# Structural instability of epitaxial zinc-blende vanadium pnictides and chalcogenides for half-metallic ferromagnets

Dan Huang,<sup>1</sup> Yu-Jun Zhao,<sup>2,a)</sup> Li-Juan Chen,<sup>2</sup> Di-Hu Chen,<sup>1</sup> and Yuan-Zhi Shao<sup>1</sup>

<sup>1</sup>*School of Physics and Engineering, Sun Yat-sen University, Guangzhou 510275, People's Republic of China*

<sup>2</sup>*Department of Physics, South China University of Technology, Guangzhou 510640, People's Republic of China*

(Received 18 December 2007; accepted 22 June 2008; published online 5 September 2008)

We present a first-principles study of the criteria governing the electronic and structural stability of epitaxial, half-metallic ferromagnetic materials with zinc-blende structure. Upon their application to vanadium pnictides and chalcogenides, we find that the criteria for structural stability are crucial when the *optimal match pattern* of an epitaxial film with the substrate is considered. Our study shows that thick zinc-blende epitaxial films are difficult to obtain by coherent epitaxial growth for vanadium pnictides and chalcogenides. We suggest that more attention needs to be paid to spin polarized ultrathin films (instead of the thick films) as high spin injection materials. © 2008 American Institute of Physics. [DOI: 10.1063/1.2973203]

## I. INTRODUCTION

Recently, many advanced spintronic devices have been designed<sup>1,2</sup> for developing next generation electronic devices. However, there is still a long way to go for practical applications other than data storage devices<sup>1</sup> mainly due to the lack of ideal spintronic materials. In addition to exploring spintronic materials by introducing magnetic ions into semiconductors, the efficient electrical injection of a highly polarized spin current into conventional semiconductors above room temperature would be a big step toward the realization of spintronic devices. Half-metallic ferromagnets (HMFs), in which one of the two spin channels is metallic, while the other has an energy gap around the Fermi energy, have attracted much attention as spin-injector materials. However, the rutile structure of CrO<sub>2</sub> (Ref. 3) and the perovskite structure of, e.g., La<sub>0.7</sub>Sr<sub>0.3</sub>MnO<sub>3</sub>,<sup>4</sup> are restricted due to low Curie temperature and low compatibility with traditional semiconductors. With the Heusler compounds such as Co<sub>2</sub>MnGe, the injected spin current polarization reportedly reaches only 27% at 2 K and decreases rapidly with increasing temperature.<sup>5</sup>

Due to their excellent properties, such as high spin polarization at high temperatures, long spin coherence length, and good compatibility with traditional semiconductors, the early transition metal (TM) pnictides and chalcogenides with a zinc-blende (ZB) structure are regarded as the most promising materials for spin injection. It is well known that, in nature, the ground states of these materials are NiAs-type or MnP-type structures rather than ZB structure. In order to obtain appropriate TM pnictides or chalcogenides with ZB structure, many investigations have been conducted through both experimental testing<sup>6–10</sup> and theoretical predictions.<sup>11–22</sup> Using a nonequilibrium method such as molecular-beam epitaxy, the ZB structures CrAs,<sup>6,7</sup> CrSb,<sup>8,9</sup> and MnAs (Ref. 10) have been fabricated as ultrathin films on the ZB structure

substrates, but no half-metallic features were observed.<sup>11</sup> Besides these three compounds, many materials, such as CrSe, VTe, CrTe, VAs, VSb, MnSb, etc., have also been predicted by a first-principles study. Most of the theoretical work<sup>12–18</sup> has been done under the isotropic expansion condition, where many of the binaries mentioned above would show half metallicity in a certain range of substrate lattice. In comparison with the isotropic expanded NiAs (or MnP) structure, the corresponding ZB structure has a good chance to be energetically favorable. However, when TM pnictides or chalcogenides are grown on the surface of semiconductor substrates, the lattice mismatch will only impose a biaxial strain, and the atomic arrangement along the other dimension will be adjusted to avoid remarkable bond length changes. Therefore, the biaxial strain models may be more useful to simulate the epitaxial growth. Some studies<sup>19–21</sup> have been done on the stability of ZB HMF under the biaxial strain models. In order to find possible thick films of binary half metals from the pseudomorphic epitaxial condition, Zhao and Zunger<sup>19</sup> calculated the epitaxial total energies of some Cr and Mn pnictides and chalcogenides, and they found that they were rarely stabilized by coherent epitaxy. Miao and Lambrecht<sup>20</sup> calculated the half-metallic properties of Cr and Mn pnictides and chalcogenides under the biaxial strain and found that the spin-flip gaps (i.e., the gaps between the lower edge of the conduction band and the Fermi energy) of the binaries were changed only slightly in different substrates.

In this paper, we attempt to further discuss the criteria for possible epitaxial HMF with a ZB structure as well as to screen a set of vanadium pnictides and chalcogenides by applying these criteria. To find a promising epitaxial HMF, we need to consider both the electronic stability and structural stability of an HMF in its ZB epitaxial phase. From the viewpoint of electronic stability, the candidate is required to have the following features in its epi-ZB phase: (i) strong ferromagnetic (FM) favored and (ii) possessing an energy gap in its minority spin channel at the available semiconductor substrate. From the view of structural stability, the candidate is

<sup>a)</sup>Author to whom correspondence should be addressed. Electronic mail: zhaoyj@scut.edu.cn.

TABLE I. The predicted lattice constants ( $\text{\AA}$ ) and magnetic moment ( $\mu_B$ ) of the vanadium pnictides and chalcogenides with the equilibrium ZB structure. Other theoretical results from the literature are also listed for comparison.

	This work		Other work	
	$a_0$ ( $\text{\AA}/\text{GGA}$ )	$\mu_B$	$a_0$ ( $\text{\AA}/\text{LDA}$ )	$a_0$ ( $\text{\AA}/\text{GGA}$ )
VS	5.365	2.29	5.24 <sup>a</sup>	
VSe	5.728	2.75	5.56 <sup>a</sup>	
VTe	6.223	3.00	6.06 <sup>a</sup>	6.271, <sup>b</sup> 6.27 <sup>b</sup>
VP	5.433	1.98	5.27 <sup>a</sup>	
VAs	5.670	2.00	5.54, <sup>a</sup> 5.6 <sup>c</sup>	5.66 <sup>d</sup>
VSb	6.161	2.00	5.98, <sup>a</sup> 6.0 <sup>c</sup>	

<sup>a</sup>Reference 12.

<sup>b</sup>References 14 and 17.

<sup>c</sup>Reference 13.

<sup>d</sup>Reference 25.

required to be (i) energetically bound as the substrate lattice changes and (ii) energetically more favorable than another epitaxial phase with an optimal interface pattern at the available substrates. While most of the issues have been discussed in Refs. 19 and 20, here we pay more attention to the universality of the weak dependence of the spin-flip gap on the substrate lattice and to the impact of an optimal interface pattern on the structural stability of epi-ZB versus epi-NiAs, exemplified by a set of vanadium pnictides and chalcogenides. The crucial role of the structural stability (particularly with the consideration of optimal interface pattern) for the epi-ZB films is also demonstrated with our extended study on CrSe and MnSb, the candidates for HMF suggested by earlier works.<sup>19,20</sup> The optimal interface pattern is also discussed with a simplified mismatching area rate model, which is found to be helpful in the structural stability study of the epi-NiAs phase.

By applying the criteria on a set of vanadium pnictides (VP, VAs, and VSb) and chalcogenides (VS, VSe, and VTe), we find that there are no significant changes of the conduction band minimum (CBM) of the minority spin relative to the Fermi level, which is consistent with the observations from Ref. 20. Furthermore, the epitaxial total energy of the ZB structure is remarkably higher than that of the NiAs structure when considering its optimal interface pattern at a different substrate region. This shows that the criteria of structural stability are stronger than those of electronic stability. In fact, the epi-ZB phase of VS, VSe, and VP does not exhibit half metallicity in a wide substrate lattice range. While VTe, VAs, and VSb show half metallicity under a wide biaxial strain range, they are not energetically stable in comparison with the epitaxial NiAs structure at their optimal interface pattern. Thus, thick films of HMFs are difficult to obtain from these vanadium pnictides and chalcogenides, and new efforts may be required to find ideal candidates. In addition, the aforementioned HMF candidates CrSe (Ref. 19) and MnSb (Ref. 20) are found to be structurally unstable in their epi-ZB phase, when considering the optimal interface match. This demonstrates the crucial role of the interface match in the structural stability of epi-ZB phases, and it makes the thick films of the epi-ZB phases virtually unreachable for the binaries of NiAs (or MnP) ground state.

## II. COMPUTATIONAL DETAILS

The calculations are conducted with the pseudopotential plane wave method within the generalized gradient approximation (GGA) of PW91 formulas<sup>22</sup> and the projector augmented wave potentials, as implemented by the VASP code.<sup>23,24</sup> The charge density is obtained from the Monkhorst–Pack  $k$ -space integration method, using a mesh of  $8 \times 8 \times 8$  for ZB and  $6 \times 6 \times 4$  for the NiAs structures, with an energy cutoff of 318.9 eV.

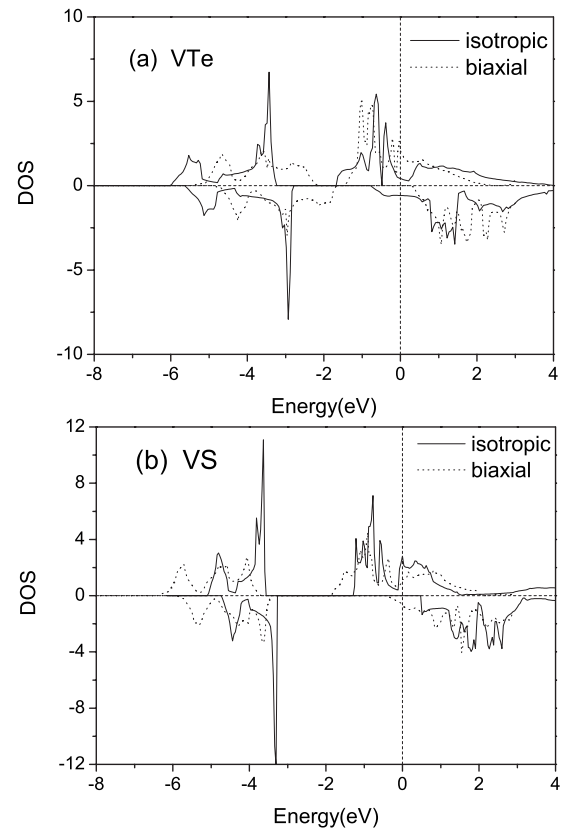


FIG. 1. Density of states (DOS) for (a) VTe and (b) VS under isotropic (solid lines) and biaxial (dashed lines) strains. The imposed isotropic and biaxial compression strains in the (001) plane are all 0.1 for VTe, but the expansion for VS. Spin-up (down) DOS is denoted by positive (negative) values, and the Fermi level is set to zero.

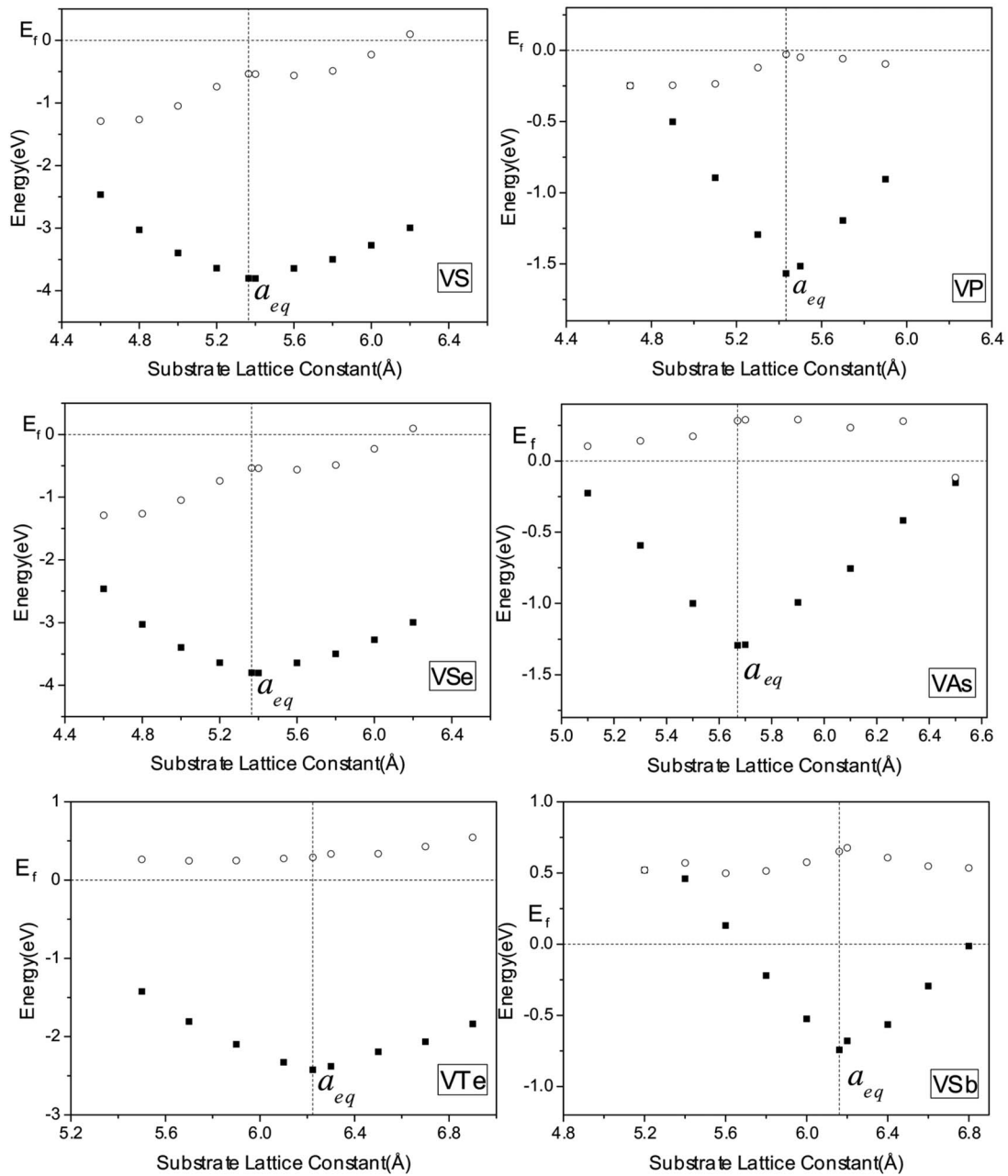


FIG. 2. Changes of the VBM (square) and CBM (circle) in the minority spin channel with respect to the substrate lattice. The Fermi level is set to zero.  $a_{eq}$  is the equilibrium lattice constant of the ZB-type structure. (The results of VP at a substrate lattice greater than 6.0 Å are not shown in the plot since it becomes paramagnetic.)

### III. RESULTS AND DISCUSSION

The equilibrium lattice constants  $a_0$  of the ideal ZB structure are listed in Table I. Our calculated results are in good agreement with other available GGA results. The GGA results are greater than the local density approximation (LDA) results by around 3% and are expected to be closer to the “real” lattice constants of the ZB TM pnictides and chalcogenides.<sup>12</sup> Under the equilibrium lattice constant, VTe, VAs, and VSb show half metallicity, while the others do not. The integer magnetic moments listed in Table I correspond to the half-metallic feature of the binaries.

Under the epitaxial growth condition, the overlayer coordinates with the substrate, i.e., the lattice constants of the in-plane axes, would decrease or increase along with the

change of substrate lattice. Assuming that the ZB binary compound growth is along the [001] direction on the substrate (a conventional semiconductor with ZB structure), we fix the  $a$  and  $b$  axes at the corresponding substrate lattice constants and then relax the  $c$  axis in our calculation. The subsequent change in half metallicity under the biaxial strain is different from the isotropic strain. Generally, if the strain is isotropic, the systems have a tendency to exhibit half metallicity on the expansion strains, even if there is no half metallicity at equilibrium. This is caused by the stronger spin splitting of the  $d$  bands, which originates from the weaker interaction between the TM atoms and the surrounding anions due to volume expansion. Similarly, the half metallicity could disappear with the isotropic compression strain. For

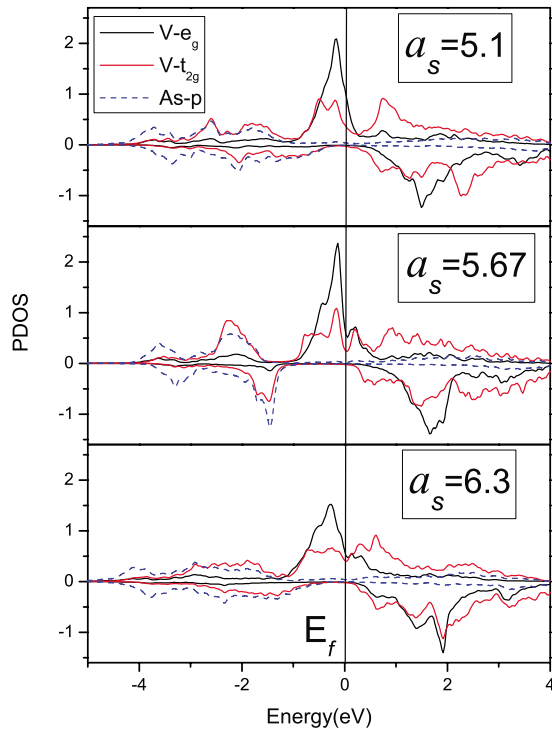


FIG. 3. (Color online) PDOS for VAs for different substrate lattices under the epitaxial growth condition.

example, under the isotropic strain, VS becomes half metallic when the substrate lattice constant is greater than 5.82 Å, and the half-metallic character of VTe would vanish if the substrate lattice constant is less than 6.10 Å.<sup>12</sup> However under the biaxial strain, the situation is different (c.f. Fig. 1): at an expansion strain of 0.1 (i.e.,  $\Delta a/a_0=0.1$ ,  $\Delta a$  is the change in the lattice constant), VS still does not show half metallicity under the biaxial expansion condition. VTe, however, keeps half metallicity even at a biaxial compression strain of 0.1 (i.e.,  $\Delta a/a_0=-0.1$ ).

In order to obtain the variation of the half metallicity with the substrate lattice, we plot the valence band maximum (VBM) and CBM of the minority spin in Fig. 2. Here, the Fermi level is determined by the majority spin channel. When the VBM of the minority spin channel is below the Fermi level and the corresponding CBM is above it, the binary compound shows half metallicity. This is the case for VTe, VAs, and VSb on most of the discussed substrate range. If this premise does not hold true, the half metallicity disap-

pears. This is the case for VS, VSe, and VP on most of the discussed substrate range. More accurate results can be obtained from Fig. 2. It shows that the CBM of the minority spin channel varies only slightly relative to the Fermi level. This is consistent with the weak dependence of the spin-flip gaps with different substrates in Cr and Mn pnictides and chalcogenides reported by Miao and Lambrecht.<sup>20</sup> The VBM moves upward to the Fermi level with any imposed biaxial strain. It is clear that the valence band is dominated by  $p$ - $d$  hybridization, while the conduction band mostly comes from the  $d$ -orbital of vanadium, as can be seen by further analysis on the partial density of states (PDOS) of VAs (c.f. Fig. 3) and VTe (not shown in Fig. 3). Since the  $d$  levels are more localized than the  $p$ - $d$  hybridization levels, the valence band is more sensitive to the strain than the conduction band is. This explains why the VBM moves upward to the Fermi level markedly, while the CBM varies only slightly. Meanwhile, we find that under the expansion strain ( $c/a < 1$ ), the  $p_z$  and  $d_{xy}$  levels are squeezed and overlapped more with their neighboring levels. As a result, the valence band width increases. Under the compression strain ( $c/a > 1$ ), the  $p_x$ - $d_{yz}$  and  $p_y$ - $d_{xz}$  levels are squeezed, and the valence band width increased as well.<sup>26</sup> The asymmetry of VBM changes with respect to  $a_{eq}$  (c.f. Fig. 2) also reflects their different electronic contributions. Our calculation also shows that vanadium chalcogenides have greater gaps than its pnictides.

So far, we have discussed the half metallicity of vanadium pnictides and chalcogenides with the ZB structure and found that VTe, VSb, and VAs have half metallicity in the FM phase around the equilibrium lattice constants. Could these ZB structures with half metallicity be stable under the epitaxial growth condition? To answer this question, we have performed the epitaxial total energy calculation for the ZB structure and the NiAs structure of both FM and antiferromagnetic (AFM) spin arrangements.

Under the epitaxial growth condition, the stability of a high-energy pseudomorphic ZB film is not decided by the energy difference  $\Delta_{bulk}$  between the isotropic deformed ZB materials and the ground state structure but rather by the energetics of the biaxial deformed film relative to the ground state,  $\Delta_{epi}$ .<sup>19</sup> The critical thickness of the ZB-like film depends on the lattice mismatch between the NiAs and ZB phases at a given substrate and the corresponding  $\Delta_{epi}$ .

The experimental and calculated lattice constants and  $c/a$  values for vanadium pnictides and chalcogenides are

TABLE II. The lattice constants and the  $c/a$  value of the NiAs-type structure of the six V pnictides and chalcogenides. The calculated magnetic properties at the ground states are also listed.

	Calculation				Experiment			Ref.
	$a$ (Å)	$c$ (Å)	$c/a$	Magnetic	$a$ (Å)	$c$ (Å)	$c/a$	
VS	3.176	6.107	1.923	PM	3.152	6.221	1.974	27
VSe	3.921	5.363	1.368	AFM	3.918	5.528	1.411	27
VTe	4.264	5.488	1.287	AFM	3.983	6.133	1.54	28
VP	3.138	6.263	1.996	PM	3.178	6.222	1.958	29
VAs	3.284	6.527	1.988	PM	...	...	...	...
VSb	4.147	5.563	1.341	FM	4.27	5.447	1.276	30

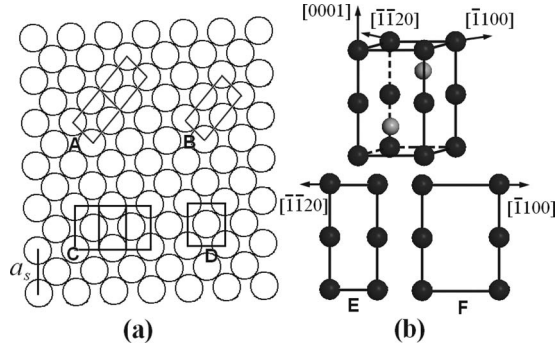


FIG. 4. The possible structural match patterns at the interface of NiAs-type and ZB-type structures. The A-D planes could be translated to other high symmetry sites with an equivalent mismatching area rate.

listed in Table II. The  $c/a$  values of VSe, VTe,<sup>31</sup> and VSb are close to 1.4, and it is close to 2.0 for VS, VP, and VAs (Ref. 32) in our calculations. Therefore, an appropriate match pattern between the film and a given substrate needs to be investigated due to the large variation of  $c/a$  values. Experimentally, some NiAs-type films, such as MnAs,<sup>33</sup> have been known to grow along the  $[1\bar{1}00]$  direction. Here, we assume that most of the atoms are initially deposited at high symmetry sites, such as top, bridge, or center, which is a general property of surface adsorption. Based on these assumptions, the NiAs  $E$  plane, with the ratio of two axes being equal to  $c/a$ , is considered to match the A, B, C planes, which have axes ratios of 1.5, 2.0, and 1.5, respectively (c.f. Fig. 4). In addition, the  $F$  plane of NiAs is considered due to its similar axes ratio with the ZB  $D$  plane when the compound has a large  $c/a$  value (i.e., close to 2.0). In different substrate lattice regions, the four possible patterns of  $E$  matching A, B, or C, and  $F$  matching  $D$  are considered in this work.

When the structures of the binaries at the interface deviate from the equilibrium, their energies will increase. The energy change is determined by the degree of mismatching and the elastic constants at the related directions. The pattern of the lowest energy would be the appropriate growth mode during the epitaxial growth. When the anisotropy of the elastic constant of the binaries is not significant, the interface patterns will be dominated by the ratio of the mismatching area,  $R_{\text{mm}}$ , which is defined as

$$R_{\text{mm}} = (S_{\text{ZB}} + S_{\text{NA}} - 2S_{\text{overlap}}) / S_{\text{NA}}. \quad (1)$$

Here,  $S_{\text{ZB}}$  is the unit area of ZB substrate, which could be the area of A, B, C, or D, as shown in Fig. 4(a);  $S_{\text{NA}}$  is the area of the NiAs phase at the interface, which could be the area of  $E$  or  $F$ , as shown in Fig. 4(b); and  $S_{\text{overlap}}$  is the overlap area of the two lattices.

The ratio of the mismatching area for VTe and VS is plotted in Fig. 5 with respect to the substrate lattice. The value of  $R_{\text{mm}}$  varies between 0.14 and 0.37 for VTe and 0.03 and 0.22 for VS in a reasonable substrate lattice range. It indicates that the matching pattern with the lowest  $R_{\text{mm}}$  shifts from the  $E$ -over- $A$  pattern to  $E$ -over- $C$  pattern as the substrate size increases for VTe. With the increasing substrate lattice constant, VS has  $E$ -over- $B$ ,  $E$ -over- $C$ , and then  $F$ -over- $D$  subsequences. The  $R_{\text{mm}}$  values of VSe and VSb (VP) have a similar configuration as VTe (VS) since VSe and

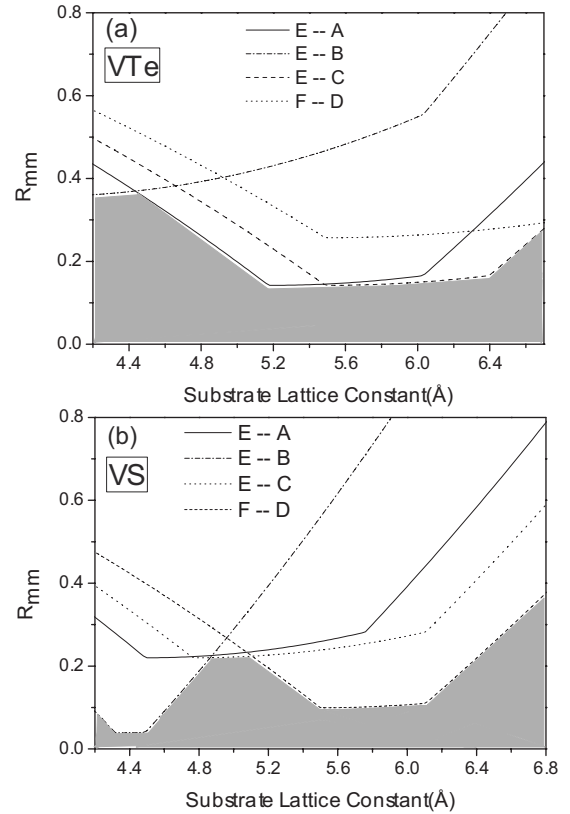


FIG. 5. The mismatching rate  $R_{\text{mm}}$  of (a) VTe and (b) VS in relation to the substrate lattice constants for different match patterns. The optimal interface match pattern is highlighted by the shadows.

VSb (VP) have a similar  $c/a$  ration in the NiAs phase as VTe (VS). The substrate lattice constant for the ZB phase being studied ranges within 85%–115% of its equilibrium lattice constant  $a_0$ .

Figure 6 shows the detailed results of the isotropic and biaxial curves in both the FM and AFM spin arrangements for these systems. For the ZB-type structures, the energy of FM is always lower than the AFM except VP on a substrate of lattice constant greater than 6.0 Å. It shows that the criterion for FM stability for the ZB vanadium pnictides and chalcogenides is rather weak and easy to realize. The biaxial curves of ZB structure are weakly bound, especially for vanadium pnictides. The biaxial curves are much flatter than the isotropic curve due to relaxation along the perpendicular direction. The biaxial energy of the ZB structure is always higher than the biaxial energy of the NiAs structure with the optimal matching pattern, in accordance with its NiAs-type ground state. The isotropic energy of the ZB structure could be lower than the isotropic energy of the NiAs structure at a certain range of the substrate lattice. The calculated epitaxial NiAs energy curves of VTe and VS show the optimal matching patterns of  $E$ -A to  $E$ -C, and  $E$ -B,  $E$ -C to  $F$ -D, respectively, as the substrate lattice increases, which is consistent with the mismatching curves in Fig. 5. It indicates that the optimal match pattern could be estimated from the ratio of the mismatching area. If we consider only one matching pattern, the epitaxial NiAs curves could be higher than the epitaxial ZB curve at a certain substrate range. For example, the  $F$ -D pattern for VS is optimal at a range around 5.7 Å,

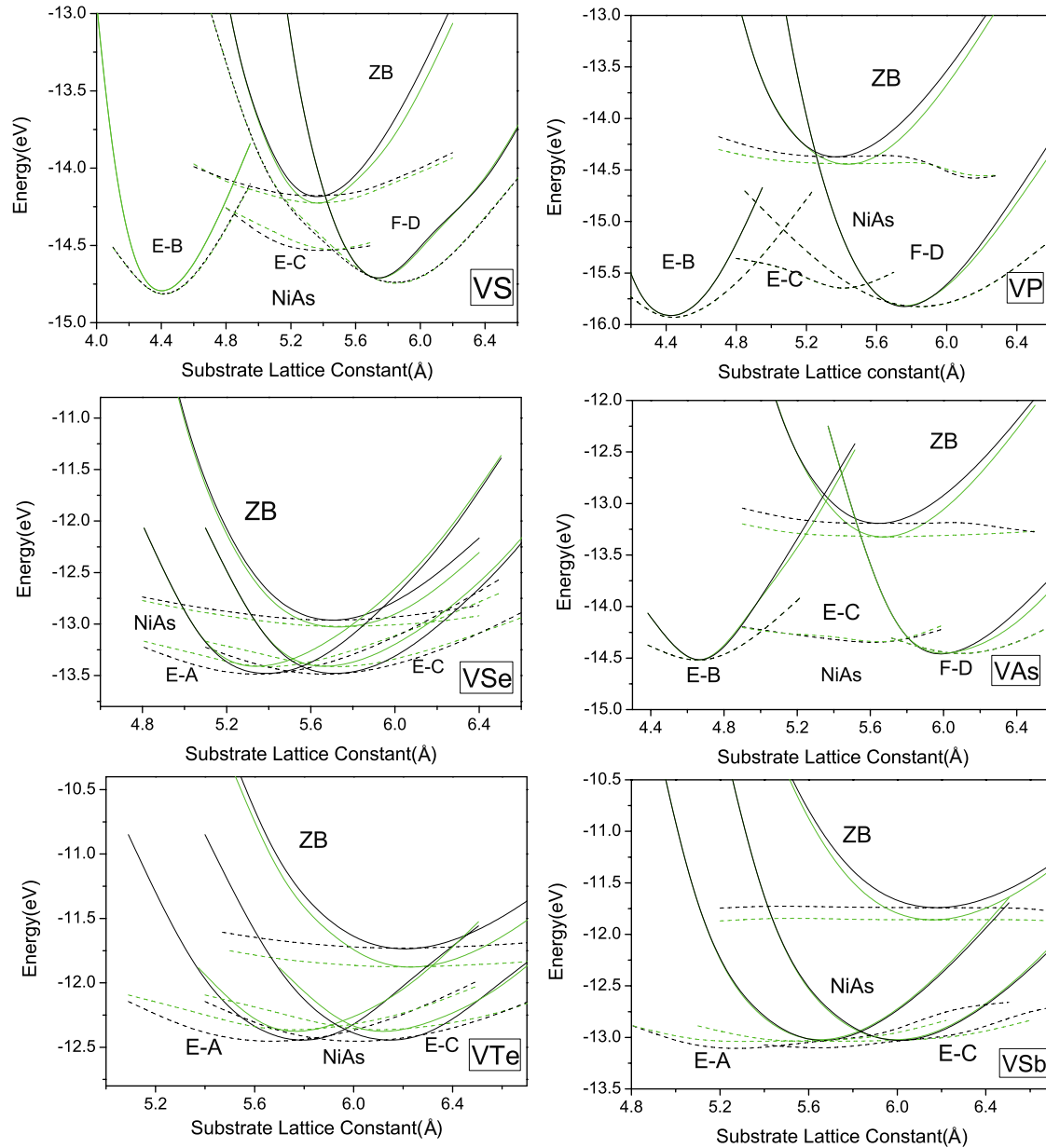


FIG. 6. (Color online) The calculated isotropic (solid lines) and biaxial (dashed lines) total energies for both ZB- and NiAs-type structures, with FM and AFM spin arrangements denoted by green and black lines, respectively. (The isotropic energies of VP, VAs, and VS are not plotted for the *E-C* pattern, which is actually a shift of another pattern along the *x* axis.)

but its energy curve is higher than the epitaxial ZB curve for substrates with a lattice smaller than 5.4 Å. For all binaries, the epitaxial NiAs energy with a *C-E* matching pattern is usually lower than the epitaxial ZB energy. This shows that the criterion for the structural stability of a ZB HMF is very strong and hard to satisfy. An extensive search of optimal matching patterns will only further reduce the structural stability of epitaxial ZB and thus will not change the conclusion. Here, the impact of the interfacial energy is not discussed when it is negligible for the thick films. The situation for ultrathin films could be different since the interfacial energy will play a much bigger role. Studies on epitaxial growth and spin injection of ultrathin film may bring new hope for a ZB HMF for high spin injection materials.

In order to further check the crucial role of the structural stability of epitaxial films (particularly with respect to the

interface match), we extend our studies to CrSe and MnSb, which are the promising candidates for HMF suggested in Refs. 19 and 20. The mismatching rates of various interface patterns for NiAs-type epitaxial films of CrSe and MnSb are plotted in Figs. 7(a) and 7(b). This suggests that the optimal match patterns are *E-A*, *E-C*, and *F-D* for CrSe, and *E-A* and *E-C* for MnSb, respectively, as the substrate lattice increases. The epitaxial energies of a NiAs-type structure of the suggested optimal interface patterns of CrSe and MnSb are calculated as well as their ZB-type isotropic energies and epitaxial energies [shown in Figs. 7(c) and 7(d)]. The optimal interface match patterns from the real calculations are consistent with the suggested patterns from the mismatching area rate plot. Figures 7(c) and 7(d) show that the epitaxial energy of a ZB structure is also significantly higher than the epitaxial energy of a NiAs structure with the optimal match-

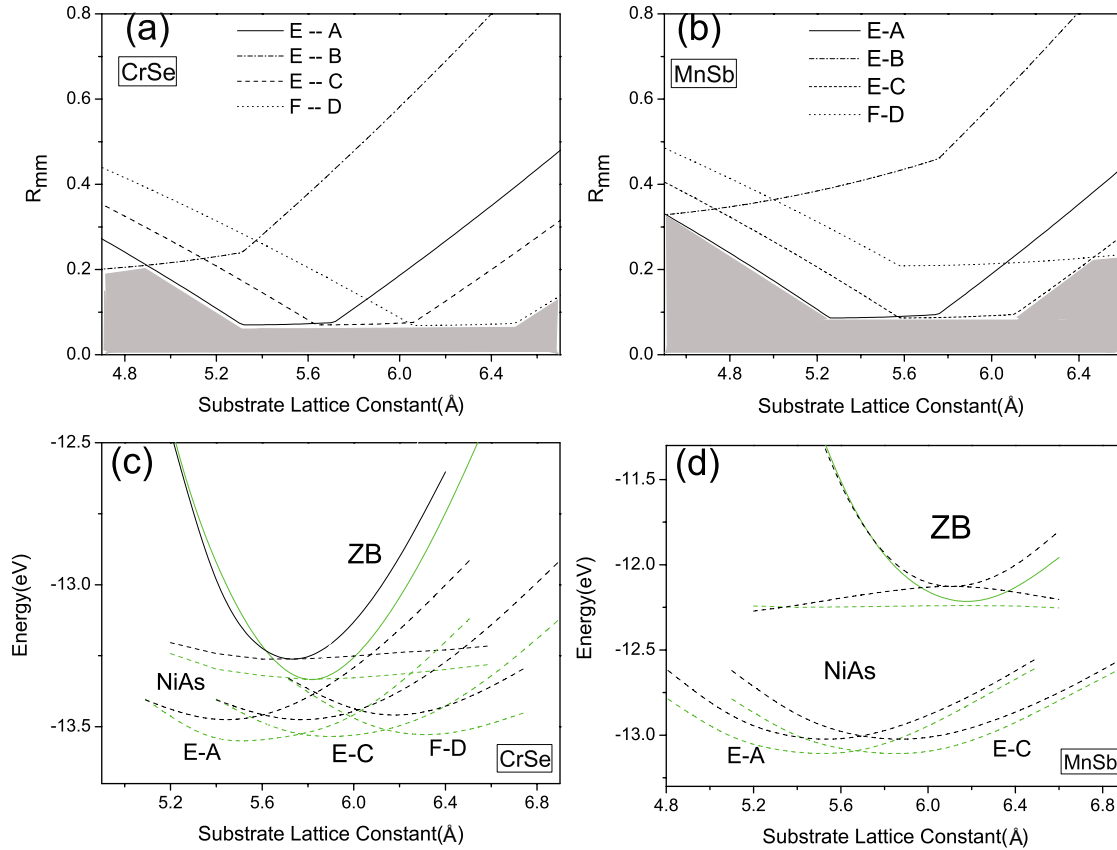


FIG. 7. (Color online) The mismatching rate  $R_{\text{mm}}$  of (a) CrTe and (b) MnSb. The calculated isotropic (solid lines) and biaxial (dashed lines) total energies of (c) CrSe and (d) MnSb for both ZB- and NiAs-type structures, with FM and AFM spin arrangements denoted by green and black lines, respectively. (The isotropic energy of NiAs-type structures is not plotted.)

ing pattern. Our earlier work<sup>19</sup> gave evidence for the structural stability of the ZB epitaxial CrSe film for substrates of lattice greater than 6.2 Å, when considering only one interface match pattern (i.e., *E* matching *A*). Unfortunately, it is found here that the ZB epitaxial CrSe film will be energetically unfavorable in comparison with the NiAs-type epitaxial film with the optimal interface pattern of *F-D* for substrates of lattice greater than 6.2 Å. Meanwhile, the ZB epitaxial MnSb was reported in Ref. 20 to always show half metallicity regardless of the substrate constant, and it could be a good candidate for ZB HMF. However, it turns out that MnSb does not satisfy the structural stability constraint either [see Fig. 7(d)].

#### IV. CONCLUSION

In summary, the electronic and structural stability of possible ZB HMF are discussed using first-principles calculations. After testing VS, VSe, VTe, VP, VAs, and VSb in this way, it is found that the FM stability criterion is easy to meet for the binaries. Epitaxial ZB VSe, VTe, and VAs systems are also half metallic for a certain range of the available substrate lattice. However, it is found that the energy of the epitaxial ZB structure is always higher than that of the epitaxial NiAs-type structure with its *optimal match pattern* to the substrate. This makes the epitaxial ZB structure difficult to stabilize, even for the cases of candidates suggested earlier, such as CrSe and MnSb. Thus, ultrathin epitaxial ZB

films need to be explored more for future spintronic devices through spin injection.

#### ACKNOWLEDGMENTS

We thank the computer time at the High Performance Grid Computer Center of South China University of Technology (SCUTGrid). This work was supported by the National Natural Science Foundation of China (NSFC) under Grant No.10704025, and by the Key Project of Chinese Ministry of Education under Grant No. 108105.

<sup>1</sup>S. A. Wolf, D. D. Awschalom, R. A. Buhrman, J. M. Daughton, S. von Molnár, M. L. Roukes, A. Y. Chtchelkanova, and D. M. Treger, *Science* **294**, 1488 (2001).

<sup>2</sup>I. Žutić, J. Fabian, and S. D. Sarma, *Rev. Mod. Phys.* **76**, 323 (2004).

<sup>3</sup>N. E. Brener, J. M. Tyler, J. Callaway, D. Bagayoko, and G. L. Zhao, *Phys. Rev. B* **61**, 16582 (2000).

<sup>4</sup>J. H. Park, E. Vescovo, H. J. Kim, and C. Kwon, *Nature (London)* **392**, 794 (1998).

<sup>5</sup>X. Y. Dong, C. Adelman, J. Q. Xie, and C. J. Palmstrom, *Appl. Phys. Lett.* **86**, 102107 (2005).

<sup>6</sup>K. Ono, J. Okabayashi, M. Mizuguchi, M. Oshima, A. Fujimori, and H. Akinaga, *J. Appl. Phys.* **91**, 8088 (2002).

<sup>7</sup>J. F. Bi, J. H. Zhao, J. J. Deng, Y. H. Zheng, S. S. Li, X. G. Wu, and Q. J. Jia, *Appl. Phys. Lett.* **88**, 142509 (2006).

<sup>8</sup>J. H. Zhao, F. Matsukura, K. Takamura, E. Abe, D. Chiba, and H. Ohno, *Appl. Phys. Lett.* **79**, 2776 (2001).

<sup>9</sup>J. J. Deng, J. H. Zhao, J. F. Bi, Z. C. Niu, F. H. Yang, X. G. Wu, and H. Z. Zheng, *J. Appl. Phys.* **99**, 093902 (2006).

<sup>10</sup>T. W. Kim, H. C. Jeon, T. W. Kang, H. S. Lee, J. Y. Lee, and S. Jin, *Appl. Phys. Lett.* **88**, 021915 (2006).

<sup>11</sup>P. Mavropoulos and I. Galanakis, *J. Phys.: Condens. Matter* **19**, 315221

- (2007).
- <sup>12</sup>I. Galanakis and P. Mavropoulos, *Phys. Rev. B* **67**, 104417 (2003).
- <sup>13</sup>M. S. Miao and W. R. L. Lambrecht, *Phys. Rev. B* **71**, 064407 (2005).
- <sup>14</sup>W. H. Xie, Y. Q. Xu, B. G. Liu, and D. G. Pettifor, *Phys. Rev. Lett.* **91**, 037204 (2003).
- <sup>15</sup>B. Sanyal, L. Bergqvist, and O. Eriksson, *Phys. Rev. B* **68**, 054417 (2003).
- <sup>16</sup>J. E. Pask, L. H. Yang, C. Y. Fong, W. E. Pickett, and S. Dag, *Phys. Rev. B* **67**, 224420 (2003).
- <sup>17</sup>W. H. Xie and B. G. Liu, *J. Phys.: Condens. Matter* **15**, 5085 (2003).
- <sup>18</sup>Y. J. Zhao, W. T. Geng, A. J. Freeman, and B. Delley, *Phys. Rev. B* **65**, 113202 (2002).
- <sup>19</sup>Y. J. Zhao and A. Zunger, *Phys. Rev. B* **71**, 132403 (2005).
- <sup>20</sup>M. S. Miao and W. R. L. Lambrecht, *Phys. Rev. B* **72**, 064409 (2005).
- <sup>21</sup>M. S. Miao and W. R. L. Lambrecht, *J. Appl. Phys.* **97**, 10C304 (2005).
- <sup>22</sup>J. P. Perdew and Y. Wang, *Phys. Rev. B* **45**, 13244 (1992).
- <sup>23</sup>G. Kresse and J. Hafner, *Phys. Rev. B* **47**, 558 (1993).
- <sup>24</sup>G. Kresse and J. Furthmüller, *Phys. Rev. B* **54**, 11169 (1996).
- <sup>25</sup>B. S. Kang, S. K. Oh, J. S. Chung, and H. J. Kang, *Thin Solid Films* **488**, 204 (2005).
- <sup>26</sup>P. Mavropoulos, I. Galanakis, and P. H. Dederichs, *J. Phys.: Condens. Matter* **16**, 4261 (2004).
- <sup>27</sup>M. Knecht, H. Ebert, and W. J. Bensch, *J. Alloys Compd.* **246**, 166 (1997).
- <sup>28</sup>U. Sondermann, *Z. Angew. Phys.* **30**, 41 (1970).
- <sup>29</sup>H. Fjellvag and A. Kjekshus, *Monatsch. Chem.* **117**, 773 (1986).
- <sup>30</sup>B. Grison and P. A. Beck, *Acta Crystallogr.* **15**, 807 (1962).
- <sup>31</sup>We note that there is a large discrepancy between experiment and theory for the magnetic state and  $c/a$  value of VTe. Interestingly, the theoretical  $c/a$  value is very close to that of experiment when the magnetic state is fixed at FM. The discrepancy will not affect our conclusion on the stability of its epitaxial ZB HMF as it favors FM in the studied substrate range.
- <sup>32</sup>The optimized NiAs-type structure is used in our calculation although a MnP-type structure is observed experimentally for VAs. The conclusion is not affected since the energy of the epitaxial NiAs-type structure is already lower than that of the ZB structure.
- <sup>33</sup>M. Yokoyama, S. Ohya, and M. Tanaka, *Appl. Phys. Lett.* **88**, 012504 (2006).